THE JOURNAL OF BIOLOGICAL CHEMISTRY VOL. 285, NO. 40, pp. 30453–30462, October 1, 2010

Cys Palmitoylation of the β Subunit Modulates Gating of the Epithelial Sodium Channel*

Received for publication, June 4, 2010, and in revised form, July 20, 2010 Published, JBC Papers in Press, July 27, 2010, DOI 10.1074/jbc.M110.151845

Gunhild M. Mueller[‡1], Ahmad B. Maarouf[‡1,2], Carol L. Kinlough[‡], Nan Sheng[‡], Ossama B. Kashlan[‡], Sora Okumura[‡], Sarah Luthy[‡], Thomas R. Kleyman[‡§3], and Rebecca P. Hughey[‡§]

From the [‡]Renal-Electrolyte Division, Department of Medicine, and the [§]Department of Cell Biology and Physiology, University of Pittsburgh, Pittsburgh, Pennsylvania 15261

The epithelial Na^+ channel (ENaC) is comprised of three homologous subunits (α, β, and γ) that have a similar topology with two transmembrane domains, a large extracellular region, and cytoplasmic N and C termini. Although ENaC activity is regulated by a number of factors, palmitoylation of its cytoplasmic Cys residues has not been previously described. Fatty acid-exchange chemistry was used to determine whether channel subunits were Cys-palmitoylated. We observed that only the β and γ subunits were modified by Cys palmitoylation. Analyses of ENaCs with mutant β subunits revealed that Cys-43 and Cys-557 were palmitoylated. *Xenopus* oocytes expressing ENaC with a β C43A,C557A mutant had significantly reduced amiloride-sensitive whole cell currents, enhanced Na^+ self-inhibition, and reduced single channel P_o when compared with wild-type ENaC, while membrane trafficking and levels of surface expression were unchanged. Computer modeling of cytoplasmic domains indicated that β Cys-43 is in proximity to the first transmembrane α helix, whereas β Cys-557 is within an amphipathic α-helix contiguous with the second transmembrane domain. We propose that β subunit palmitoylation modulates channel gating by facilitating interactions between cytoplasmic domains and the plasma membrane.

Epithelial sodium channels (ENaCs)[4] mediate amiloride-sensitive Na^+ transport across the apical membrane of high resistance epithelia and have important roles in regulating extracellular fluid volume and blood pressure, as well as airway surface liquid volume and mucociliary clearance. The α, β, and γ subunits of ENaC are members of the ENaC/Degenerin family of ion channels, which include H^+-gated channels (referred to as acid-sensing ion channels (ASICs)) that are expressed in mammalian central and peripheral nervous systems and have a role in nociception and mechanosensation (1). ENaC and other family members are ion channels composed of subunits that have a similar topology with two transmembrane helices, a large extracellular region, including numerous conserved disulfide bridges, and cytoplasmic N and C termini. The recently resolved crystal structure of ASIC1 (2) revealed a homotrimer with highly organized extracellular regions, suggesting that ENaC is an $\alpha_1\beta_1\gamma_1$ heterotrimer.

ENaCs are assembled within the endoplasmic reticulum (ER), where they undergo *N*-linked glycosylation. Assembly is inefficient, and the majority of newly synthesized subunits undergo ER-associated degradation with a half-life of 1–2 h as determined by metabolic labeling (3–7). A small pool of newly synthesized subunits has a significantly longer half-life (>4 h) and represents assembled channels that have exited the ER and are present in later compartments. This latter pool contains subunits whose *N*-glycans have undergone both Golgi-dependent terminal processing and cleavage of α and γ by furin, a protease localized primarily to the *trans*-Golgi network (5, 8, 9). ENaC exit from the ER is regulated by a signal within the C-terminal cytoplasmic domain of the α subunit (αRSRYW620 in murine ENaC) that resembles the well described cytoplasmic dibasic motifs recognized by the coat protein complex II prebudding (7). Interestingly, some fraction of ENaC reaches the cell surface lacking Golgi-associated processing: the *N*-glycans are not processed, and the α and γ subunits are not cleaved (11). Proteolytic cleavage of ENaC by furin, and by other proteases in the post-Golgi compartment(s) under normal and pathological states, activates the channel by releasing small inhibitory peptides from α and γ, respectively, and thereby increasing channel open probability (P_o) (for review, see Refs. 12–17).

Ubiquitination of ENaC by Nedd4-2 and de-ubiquitination of ENaC by UCH-L3 or Usp2–45 differentially regulate ENaC membrane trafficking after reaching the cell surface, and prolonged residence on the cell surface further activates the channel by increasing subsequent proteolysis (18–20). ENaC channel gating and membrane trafficking are also regulated by inositol phospholipids presumably by binding cationic residues within the β and γ subunits (21–25; for review, see Ref. 26).

Post-translational modification of channels by Cys palmitoylation is another potential mechanism for modulating ENaC activity. In mammals, there are 23 members of the palmitoyltransferase family, also known as DHHC Cys-rich domain-containing proteins (or "DHHC proteins"), which catalyze the

* This work was supported, in whole or in part, by National Institutes of Health Grants DK65161 (to T. R. K. and R. P. H.) and DK079307 (Pittsburgh Center for Kidney Research).

[1] Both authors contributed equally to this work.

[2] Supported by a postdoctoral fellowship award from the American Heart Association.

[3] To whom correspondence should be addressed: Renal-Electrolyte Division, Dept. of Medicine, University of Pittsburgh School of Medicine, A919 Scaife Hall, 3550 Terrace St., Pittsburgh, PA 15261. Tel.: 412-647-3121; Fax: 412-648-9166; E-mail: kleyman@pitt.edu.

[4] The abbreviations used are: ENaC, epithelial Na^+ channel; IP, immunoprecipitate; I_{peak}, peak current; I_{ss}, steady-state current; M1, first transmembrane domain; M2, second transmembrane domain; maleimide-PEO_2-biotin, (+)-biotinyl-3-maleimidopropionamidyl-3,6-dioxaoctanediamine; MDCK, Madin-Darby canine kidney; MTSET, [2-(trimethylammonium)ethyl]-methanethiosulfonate bromide; P_o, open probability; pS, picosiemens; ASIC, acid-sensing ion channel; ER, endoplasmic reticulum; SSI, Na^+ self-inhibition.

palmitoylation of proteins at specific cytoplasmic Cys residues (27, 28). DHHC refers to the conserved reactive site residues (Asp-His-His-Cys) found in all palmitoyltransferases. Cys palmitoylation of proteins is often found near hydrophobic moieties, including (i) C-terminal prenyl groups, (ii) N-terminal myristoyl groups, (iii) other palmitoylated Cys residues, and (iv) transmembrane domains (29). Transient Cys palmitoylation of soluble cytoplasmic proteins may reversibly enhance their membrane association by providing an acyl group and thereby increasing hydrophobicity. The subcellular localization of specific palmitoyltransferases determines their target membrane for soluble protein substrates (for reviews, see Refs. 28, 29). Recent reports indicate that subcellular localization of palmitoyltransferases also provides the functional setting for modification of transmembrane proteins (30).

Cys palmitoylation has a primary or secondary role in ER quality control. This modification is essential for the proper folding and ER exit of several multitransmembrane proteins (31–35). Transient palmitoylation also differentially regulates membrane trafficking of proteins at the cell surface. For example, Cys mutations that block palmitoylation (i) inhibit endocytosis of the asialoglycoprotein receptor (36), (ii) stimulate endocytosis (but not recycling) of the transferrin receptor (37), and (iii) inhibit recycling (but not endocytosis) of the transmembrane mucin MUC1 (38). Mutations that prevent Cys palmitoylation also (i) block interactions of tetraspanin CD151 with integrin $\alpha6\beta4$ (39), (ii) block association of the netrin-1 receptor with lipid microdomains (40), and (iii) alter the function of several G-protein-coupled receptors (34, 41). Palmitoylation of the Kv1.1 channel facilitates K^+ channel interactions with plasma membrane lipids, which contributes to electric field-induced conformational changes (42). Clearly, Cys palmitoylation has a key role in modulating the membrane trafficking and activity of many transmembrane proteins.

Using fatty acid-exchange chemistry we found that the β and γ ENaC subunits, but not the α subunit, are modified by Cys palmitoylation. Although there are five cytoplasmic Cys residues in the β subunit, we found that only the Cys adjacent to the first and second transmembrane domains are palmitoylated. Expression of ENaC with a mutant β subunit lacking these two Cys exhibited reduced amiloride-sensitive currents when expressed in *Xenopus* oocytes. Analysis of ENaC membrane trafficking, surface levels (N), and single channel recordings showed that the reduction in ENaC activity reflected a lower channel P_o. Our results suggest that Cys palmitoylation of the β subunit modulates channel gating, perhaps by stabilizing the open state of the channel.

EXPERIMENTAL PROCEDURES

Vectors and Cell Culture—Wild-type (WT), and N-terminal and C-terminal epitope-tagged mouse ENaC subunit cDNAs, were previously described (8, 43). The β subunit mutations were generated in pCDNA3.1(+) (Invitrogen) using a standard two-step PCR method. MDCK type 1 cells were a gift from Barry M. Gumbiner (Memorial Sloan-Kettering Cancer Center, New York) and MDCK type 2 cells were obtained from Gerard Apodaca (University of Pittsburgh, Pittsburgh, PA). Cells were cultured and transfected with ENaC cDNAs as previously described (8).

Assay for Protein Cys Palmitoylation in MDCK Cells—Cys palmitoylation of ENaC subunits was assessed using fatty acid-exchange chemistry whereby *S*-palmitate is selectively removed by treatment with hydroxylamine and exchanged for biotin (44, 45). We optimized conditions for assaying ENaC palmitoylation. $\alpha\beta\gamma$ENaC was transiently expressed in MDCK (type 1 or type 2) cells, where the α, β, or γ subunit had both an N-terminal HA tag and a C-terminal V5 tag, and the other two subunits lacked epitope tags. Cells were plated at 90% confluency on plastic (24-mm well of a 12-well Costar Cluster, Corning, NY) the day before transfection with plasmids and Lipofectamine 2000 (Carlsbad, CA). The day after transfection, cells were extracted for 20 min at room temperature on a rotating shaker using 200 μl of detergent buffer (50 mM Tris-HCl, pH 8, 4 mg/ml deoxycholate, 1% Nonidet P-40) containing 50 mM *N*-ethylmaleimide to alkylate free Cys residues. Cell debris was removed by centrifugation at 20,800 $\times$ *g* for 7 min at 4 °C. The supernatant was recovered, and ENaC was immunoprecipitated (IP) in a 1.5-ml micro tube (with snap cap) with 10 μl of goat anti-V5 antibodies immobilized on agarose (Bethyl Laboratories, Inc., Montgomery, TX) by incubation overnight at 4 °C with end-over-end mixing. 20 μl of Sepharose CL6 beads were then added as carrier to each IP. The IPs were washed twice with 1% Triton X-100 in HEPES buffer (10 mM HEPES, pH 7.4, 150 mM NaCl) and once with HEPES buffer, by vortexing and centrifuging at room temperature twice for 0.5 min at 9,300 $\times$ *g* and removing all liquid with a Hamilton syringe (0.1 ml Gastight #1710, 22 s, inner diameter 0.71 mm, Hamilton Co., Reno, NV). IPs were resuspended into 0.5 ml of either 1 M hydroxylamine-HCl (pH 7.4, 150 mM NaCl, 0.2% Triton X-100) to remove *S*-palmitate or 1 M Tris-HCl (pH 7.4, 150 mM NaCl, 0.2% Triton X-100) as a control. The tubes were rotated end-over-end at room temperature for 60 min and centrifuged at room temperature, and all liquid was removed with a Hamilton syringe. Pellets were washed twice with 1% Triton X-100 in HEPES buffer and resuspended in 0.5 ml of 0.2 mg/ml EZ-Link® (+)-biotinyl-3-maleimidopropionamidyl-3,6-dioxaoctanediamine (maleimide-PEO2-biotin from Thermo Scientific, Rockford, IL) in 50 mM Tris-HCl, pH 7, 150 mM NaCl, and 0.2% Triton X-100) to label newly exposed Cys sulfhydryls. Tubes were incubated at room temperature with end-over-end rotation for 2 h before washing twice with 0.01% SDS in HEPES buffer, and all liquid was removed with a Hamilton syringe. ENaC was released from the beads by adding 60 μl of 1% SDS HEPES buffer and heating at 90–100 °C for 2 min. The tubes were centrifuged at room temperature, and the supernatant was recovered with a Hamilton syringe and moved to a new tube. 10% was removed to determine the "Total IP," and the remainder was mixed with 0.8 ml of 0.5% Triton X-100 in HEPES buffer and 30 μl of Streptavidin-conjugated agarose to recover the newly biotinylated ENaC. The samples were incubated overnight with end-over-end rotation at 4 °C and then washed with 1% Triton X-100 in HEPES buffer followed by one wash with HEPES buffer. All liquid was removed with a Hamilton syringe, and the pellet was incubated for 3.5 min at 90–100 °C with Laemmli sample buffer (Bio-Rad) plus 0.7 M

β-mercaptoethanol, and the precipitated proteins were analyzed by SDS-PAGE and immunoblotting with either mouse anti-V5 antibodies conjugated to horseradish peroxidase (Invitrogen) or mouse anti-V5 antibodies (Invitrogen) and goat anti-mouse second antibody conjugated to horseradish peroxidase. Bands were visualized using Western Lightning Chemiluminescence Reagent Plus (PerkinElmer Life Sciences) and quantified with a Bio-Rad Versadoc (Bio-Rad) and Bio-Rad Quantity One software. The percentage of biotinylated subunit was calculated for each sample based on the total IP. The difference in the percentage of biotinylated subunit following hydroxylamine treatment, and the percentage of biotinylated subunit following Tris treatment (*i.e.* control) represents the percentage of the subunit that was palmitoylated.

Functional Expression and Biochemistry in Xenopus Oocytes—ENaC expression in *Xenopus* oocytes, two-electrode voltage clamp and chemiluminescent surface detection of ENaC were performed as previously reported (46–48). Oocytes were injected with WT α and γ, along with WT or mutant β cRNAs (1–2 ng of each), and electrophysiological measurements were performed 24 h post-injection. The difference in measured current at −100 mV in the absence and presence of amiloride (10 μM) was used to define ENaC-mediated currents. The protocol for harvesting oocytes from *Xenopus laevis* was approved by the University of Pittsburgh's Institutional Animal Care and Use Committee.

Membrane Trafficking in Xenopus Oocytes—ENaC exocytosis and endocytosis in *Xenopus* oocytes were determined as previously described (47, 49, 50). Biotinylation of cell-surface proteins expressed in oocytes and immunoblot analysis of biotinylated ENaC was previously described (51, 52). Briefly, channel endocytosis was determined by measuring the time-dependent loss of cell Na^+ currents in the presence of brefeldin A to block forward channel trafficking. Channel exocytosis was performed using an amiloride-binding site mutant αS583C. Surface channels with αS583C are blocked by treatment with 1 mM [2-(trimethylammonium)ethyl]methanethiosulfonate bromide (MTSET). The initial rate of current recovery reflects the rate of channel exocytosis. As these channels are relatively insensitive to amiloride, 100 μM benzamil was used to block ENaC and determine the ENaC-insensitive component of the whole cell Na^+ current.

Sodium Self-inhibition—To evaluate Na^+ self-inhibition (SSI), a low [Na^+] bath solution (1 mM NaCl) was rapidly replaced by a high [Na^+] bath solution (110 mM NaCl) while the oocytes expressing ENaC subunits were continuously clamped at −100 mV. The peak current (I_{peak}) and steady-state current (I_{ss}) were determined as previously described (53). The ratio I_{ss}/I_{peak} was used as a measure of the Na^+ self-inhibition response, with a smaller value indicating greater Na^+ self-inhibition.

Single Channel Recordings—Patch clamp was performed in oocytes expressing WT or mutant ENaCs as previously described (54, 55). Both pipette and bath solutions were the same as the high [Na^+] solution for testing Na^+ self-inhibition (110 mM NaCl). Patch clamp with a cell-attached configuration was performed using a PC-One Patch Clamp amplifier (Dagan Corp., Minneapolis, MN) and a DigiData 1322A interface connected to a PC. Patches were clamped at membrane potentials (negative value of pipette potentials) of −40 to −100 mV. Software pClamp 8 or 10 (Molecular Devices Corp./MDS Analytical Technologies) was used for data acquisition and analyses. Single-channel recordings were acquired at 5 kHz, filtered at 300 Hz by using a built-in, four-pole, low pass Bessel filter. P_o was estimated by single-channel search function of pClamp 10 from 5-min recordings that contained only 2 current levels (closed and open states) at a clamping membrane potential of −100 mV. Single-channel conductance was obtained by linear-fitting unitary currents against clamping voltages in the range of −40 and −100 mV. Unitary currents were determined by averaging multiple cursor measurements at each voltage.

Statistical Analyses—Comparisons between groups were performed with Student's *t* tests. A p value of <0.05 was considered significantly different.

RESULTS

ENaC Is Palmitoylated on the β and γ Subunits—Palmitoylation occurs primarily on cytoplasmic Cys residues, and there are five cytoplasmic Cys residues within the α subunit, five within β, and two within γ. Cys palmitoylation of ENaC subunits was assessed using fatty acid-exchange chemistry whereby *S*-palmitate, selectively removed by treatment with hydroxylamine, is exchanged for biotin (44, 45). ENaC was transiently expressed in MDCK cells, where α, β, or γ had both an N-terminal HA tag and a C-terminal V5 tag, but the other two subunits lacked tags. Cells were extracted in detergent in the presence of *N*-ethylmaleimide to alkylate free Cys sulfhydryl groups, and ENaC was immunoprecipitated with a goat anti-V5 antibody conjugated to beads. The IPs on beads were treated with 1 M hydroxylamine to release palmitate from Cys (or 1 M Tris as a control), prior to treatment with maleimide-PEO2-biotin to biotinylate newly exposed Cys sulfhydryl groups. Ten percent of each treated IP was reserved to quantify total ENaC within the sample, and the remainder was incubated with streptavidin-conjugated beads to recover biotinylated (*i.e.* palmitoylated) subunits. Both the immature (endoglycosidase H-sensitive and not cleaved) and mature (endoglycosidase H-resistant and cleaved) forms of each subunit were detected by quantitative immunoblotting with anti-V5 antibodies conjugated to horseradish peroxidase using a Bio-Rad Versadoc (Fig. 1*A*). The percentage of biotinylated subunit was determined for samples treated with either hydroxylamine or Tris. The difference in extent of subunit biotinylation following hydroxylamine *versus* Tris treatment represents the percentage of the subunit that is palmitoylated (Fig. 1*B*). Greater levels of β and γ (but not α) subunit biotinylation after treatment with hydroxylamine (*versus* Tris) were observed, consistent with Cys palmitoylation of the β and γ subunits. We observed that 14 ± 0.2% of β subunits and 8.8 ± 0.4% of γ subunits were palmitoylated (mean ± S.E. for $n = 3$ experiments).

ENaCs Lacking Sites for β Subunit Palmitoylation Exhibit Reduced Activity—The five cytoplasmic Cys residues in the β subunit were individually mutated to Ala (βC10A, βC30A, βC43A, βC557A, and βC595A), and palmitoylation of these epitope-tagged mutants was assessed when co-expressed with

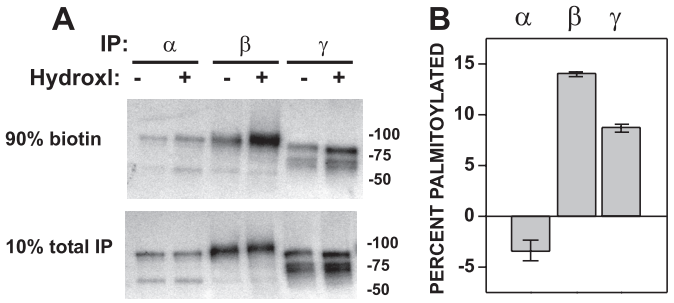

FIGURE 1. **Mouse ENaC β and γ subunits are Cys-palmitoylated.** *A* and *B*, αβγENaC with one double epitope-tagged subunit (N-terminal HA and C-terminal V5) expressed in MDCK cells was analyzed by fatty acid-exchange chemistry to replace Cys-palmitate with biotin after treatment of the IP with hydroxylamine (*Hydroxl*) (+), or with Tris (−) as a control. Biotinylated ENaC was recovered from anti-V5 IPs with streptavidin beads (*90% biotin*), and percent biotinylated was calculated from total (*10% total IP*) ENaC after quantitative immunoblotting for V5. Percent palmitoylated was calculated by subtracting percent biotinylated after treatment with Tris from that after treatment with hydroxylamine. A representative immunoblot is shown in *A*, and the data from three experiments are presented in *B* as mean ± S.E.

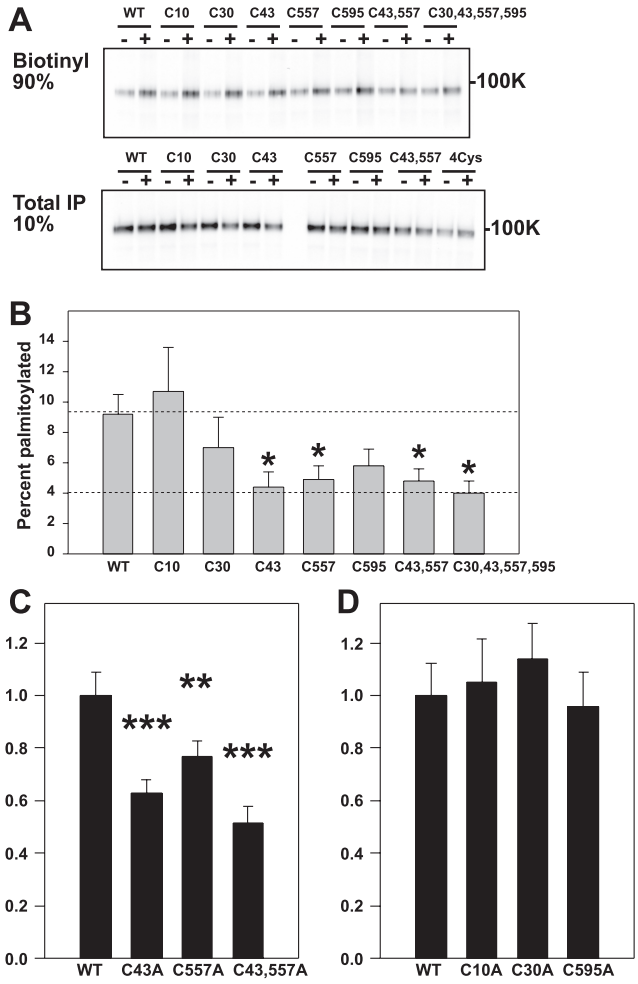

FIGURE 2. **ENaCs lacking sites for β subunit Cys palmitoylation exhibit reduced activity.** *A* and *B*, one or multiple cytoplasmic Cys in β were mutated to Ala and assessed for palmitoylation as described for Fig. 1. A representative immunoblot is shown in *A*, and combined data are presented in *B*. The percentage of β subunit palmitoylation was significantly reduced for the single mutants βC43A and βC557A when compared with WT and was not reduced further with a double βC43A,C557A mutant or a quadruple βC30A,C43A,C557A,C595A mutant (mean ± S.E., *, $p < 0.05$ *versus* WT, n = 7–20 experiments). *C*, whole cell Na^+ currents in *Xenopus* oocytes were reduced for channels with a βC43A mutant, a βC557A mutant, or a βC43A,C557A mutant, compared with WT (mean ± S.E.; **, $p < 0.01$; ***, $p < 0.001$ *versus* WT (n = 34–37 oocytes)). *D*, whole cell Na^+ currents in *Xenopus* oocytes were not significantly different for channels with a βC10A mutant, a βC30A mutant, or a βC595A mutant, compared with WT (n = 15–16 oocytes).

non-tagged WT α and γ (Fig. 2, *A* and *B*). We observed that palmitoylation of either βC43A or βC557A was significantly reduced when compared with WT β. Levels of palmitoylation of the double mutant βC43A,C557A and a quadruple mutant βC30A,C43A,C557A,C595A were similar to that observed with the single βC43A or βC557A mutants, representing background labeling of ~4% of the total β subunit pool. In contrast, biotin labeling of the WT β subunit was 9.2 ± 1.3% of the total β subunit pool (mean ± S.E. for n = 7–20 experiments). Altogether, these results indicated that ENaC is palmitoylated both on βCys-43 at the junction of the N-terminal cytoplasmic domain and the first transmembrane domain (M1), and on βCys-557 near the junction of the C-terminal cytoplasmic domain and the second transmembrane domain (M2).

We examined whether the βC43A,C557A mutant affected ENaC activity. Whole cell amiloride-sensitive currents were measured in *Xenopus* oocytes expressing either (i) WT ENaC, (ii) αβC43Aγ, (iii) αβC557Aγ, or (iv) αβC43A,C557Aγ. Currents were significantly reduced in oocytes expressing either single or double β subunit Cys mutation(s), although the βC43A and βC43A,C557A mutants reduced whole cell currents to similar levels (Fig. 2*C*). Whole cell amiloride-sensitive currents in oocytes expressing (i) αβC10Aγ, (ii) αβC30Aγ, or (iii) αβC595Aγ were not significantly different from currents in oocytes expressing WT ENaC (Fig. 2*D*).

ENaC Lacking βC43,557 Palmitoylation Exhibit Normal Surface Expression and Membrane Trafficking—Palmitoylation of the β subunit adjacent to the transmembrane domains could modulate channel activity by either altering the number of surface channels (N) by affecting membrane trafficking and/or by altering channel P_o. Three different assays were used to assess levels of surface expression of WT and αβC43A,C557Aγ channels. Oocytes expressing ENaC with WT β or mutant βC43A,C557A (24–48 h post-injection of cRNA) were subjected to: (i) surface biotinylation of ENaC, or (ii) antibody-based surface chemiluminescence detection of ENaC. Alternatively (iii) amiloride-sensitive currents were assessed using the βS518K degenerin mutation (*i.e.* αβS518Kγ *versus* αβS518K, C43A,C557Aγ), because ENaC is fully activated with the βS518K degenerin mutation. Concurrently, we measured rates of ENaC exocytosis and endocytosis to identify any effects of βC43A,C557A mutations on ENaC trafficking.

Oocyte surface biotinylation was carried out as previously described (52). Briefly, oocytes expressing ENaC with C-terminal V5-tagged WT β or mutant βC43A,C557A were treated with membrane-impermeant sulfo-NHS-SS-biotin prior to extraction with detergent and recovery of biotinylated proteins with streptavidin-conjugated agarose. Five percent of the extract was retained for immunoprecipitation with anti-V5 antibodies and represented the total cellular pool of the β subunit. Quantitative immunoblot analyses of all samples using a Bio-Rad Versadoc revealed that there was no significant differ-

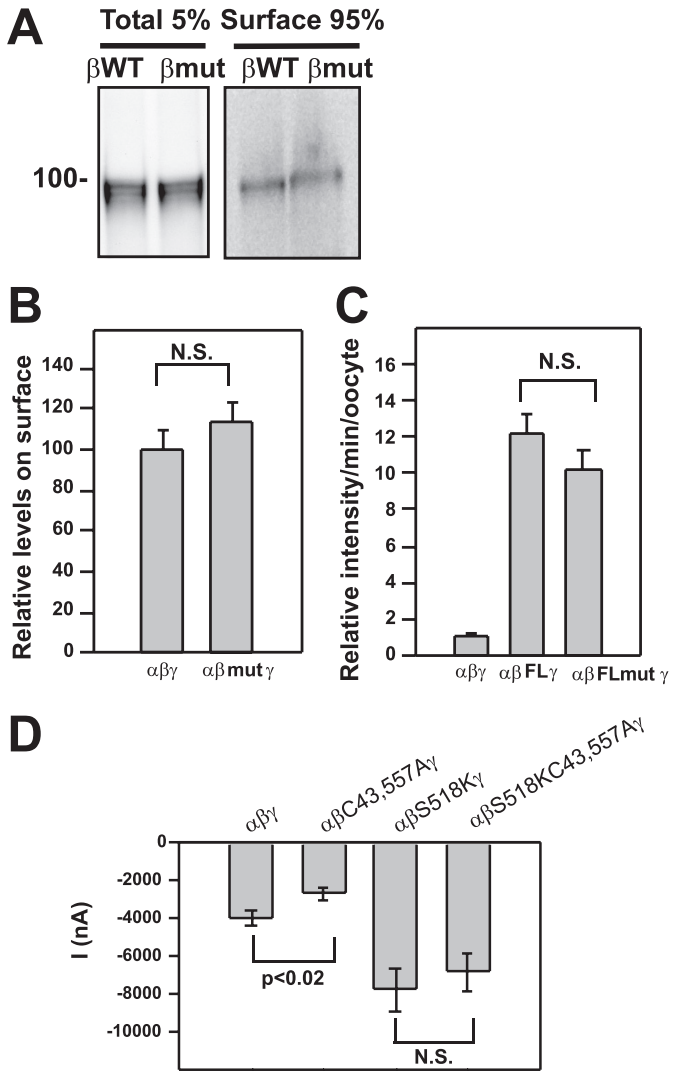

FIGURE 3. **The βC43A,C557A mutation does not affect surface expression of ENaCs.** *A* and *B*, oocytes were injected with cRNA for WT αγ and either WT β (*βWT*) or the βC43A,C557A mutant (*βmut*) with epitope tags (N-terminal HA and C-terminal V5). After surface biotinylation, an aliquot of total extract (*Total 5%*) and ENaC recovered with streptavidin-conjugated beads (*Surface 95%*) were subjected to immunoblotting with anti-V5 antibodies. A representative blot is shown in *A* ($n = 40$ oocytes each). The normalized data from four experiments (1–3 frogs each, and 9–40 oocytes per group) are presented in *B* with surface levels of WT αβγ set at 100 (± 8.3 S.E., $n = 4$). There was no significant (*N.S.*) difference between surface expression of ENaC with WT β and ENaC with mutant βC43A,C557A (113 ± 10, mean and S.E., $n = 4$). *C*, oocytes were injected with cRNA for WT αγ and either WT β or the mutant βC43A,C557A (*βmut*) with a FLAG epitope tag (*FL*) within the extracellular loop. Non-tagged ENaC was used as a negative control (αβγ). Surface levels of FLAG-tagged ENaC were subsequently determined by an antibody-based chemiluminescence assay. The data from two experiments are presented ($n = 8$–35 oocytes each group) and were normalized to non-tagged αβγENaC set at 1 (± 0.1, S.E., $n = 38$). There was no significant difference between measurements for αβFLγ (12.3 ± 1.0, $n = 52$) and αβFLmutγ (10.0 ± 0.1, $n = 47$). *D*, oocytes were injected with cRNA for WT α and γ, and either WT β, βS518K (degenerin mutant), βC43A,C557A, or βS518K, C43A,C557A. Data for amiloride-sensitive Na^+ currents are presented from three experiments ($n = 4$–7 oocytes each). A significant difference was found between αβγ (−3957 nA ± 388, mean ± S.E., $n = 18$) and αβC43A,C557Aγ (−2657 nA ± 332, $n = 16$) (*, $p < 0.02$), whereas there was no significant (*N.S.*) difference when channel P_o was enhanced by the βS518K mutation (−7797 nA ± 1173, $n = 19$ for αβS518Kγ, and −6847 nA ± 996, $n = 22$ for αβS518K, C43A,C557Aγ).

ence in the fraction of biotinylated β subunit on the cell surface when ENaC palmitoylation was blocked by the βC43A,C557A mutation (Fig. 3, *A* and *B*).

Chemiluminescence detection of surface ENaC was carried out as previously described (47). Briefly, oocytes expressing ENaC with a WT β subunit or mutant βC43A,C557A (both the WT and mutant β subunits contained an external FLAG-epitope tag) were incubated for 1 h on ice with an anti-FLAG antibody and then an HRP-tagged second antibody. Individual oocytes were placed in chemiluminescence reagent for 1 min at room temperature prior to quantitation with a luminometer (Fig. 3*C*). Oocytes expressing ENaC with a non-epitope-tagged β were used as a negative control. No significant difference in the level of chemiluminescence was observed when β subunit palmitoylation was blocked with the βC43A,C557A mutation.

Amiloride-sensitive Na^+ currents were measured in oocytes expressing ENaC with a βS518K degenerin mutation that increases the P_o to ~1 (56). The βC43A,C557A mutations were also introduced onto this βS518K background. No significant difference in whole cell amiloride-sensitive Na^+ current was observed due to the βC43A,C557A mutant in the presence of the activating degenerin mutation (57), in contrast to the significant reduction in channel activity that was observed between WT ENaC and channels lacking β subunit palmitoylation due to the βC43A,C557A mutant ($p < 0.02$) in the absence of the activating degenerin mutation (Fig. 3*D*).

Concurrently, we measured the rates of exocytosis and endocytosis of ENaC with a WT β subunit or the βC43A,C557A mutant in oocytes using our published protocols (50). Membrane-impermeant MTSET irreversibly blocks ENaCs at the cell surface when channels have an αS583C mutation (58). Briefly, ENaC exocytosis was measured by treating oocytes expressing ENaC αS583Cβγ or αS583Cβ C43A,C557Aγ, with 1 mM MTSET for 4 min to inhibit surface channels. After removing MTSET from the bath, amiloride-sensitive Na^+ currents were measured by two-electrode voltage clamp every 30 s for 5 min to monitor current recovery. The rates of recovery were similar for ENaC with WT β or the βC43A,C557A mutant (Fig. 4*A*).

ENaC endocytosis was determined by measuring amiloride-sensitive Na^+ currents in oocytes expressing αβγ or mutant αβC43A,C557Aγ, before and 1.5 and 3 h after the initiation of incubation with brefeldin A to block delivery of newly synthesized ENaC to the cell surface. We observed a similar decay of whole cell amiloride-sensitive Na^+ currents with oocytes expressing WT ENaC or the αβC43A,C557Aγ mutant, indicating that rates of endocytosis were similar (Fig. 4*B*).

ENaC Lacking Sites for β Subunit Palmitoylation Exhibit Reduced Channel P_o—As WT and αβC43A,C557Aγ channels are expressed at the cell surface at similar levels, the reduced channel activity we observed with the βC43A,C557A mutant is likely due to a reduced channel P_o. Na^+ self-inhibition reflects a reduction in channel activity in the presence of a high external [Na^+]. We have previously shown that ENaC P_o correlates with the degree of Na^+ self-inhibition; the greater the extent of Na^+ self-inhibition, the lower the channel P_o (53). We assessed the Na^+ self-inhibition response of WT channels and the mutant (αβC43A,C557Aγ) lacking sites for β subunit palmitoylation, by monitoring whole cell Na^+ currents in oocytes bathed in a low [Na^+] solution (1 mM NaCl), which was rapidly changed to a high [Na^+] bath solution (110 mM NaCl) (Fig. 5*A*). Following

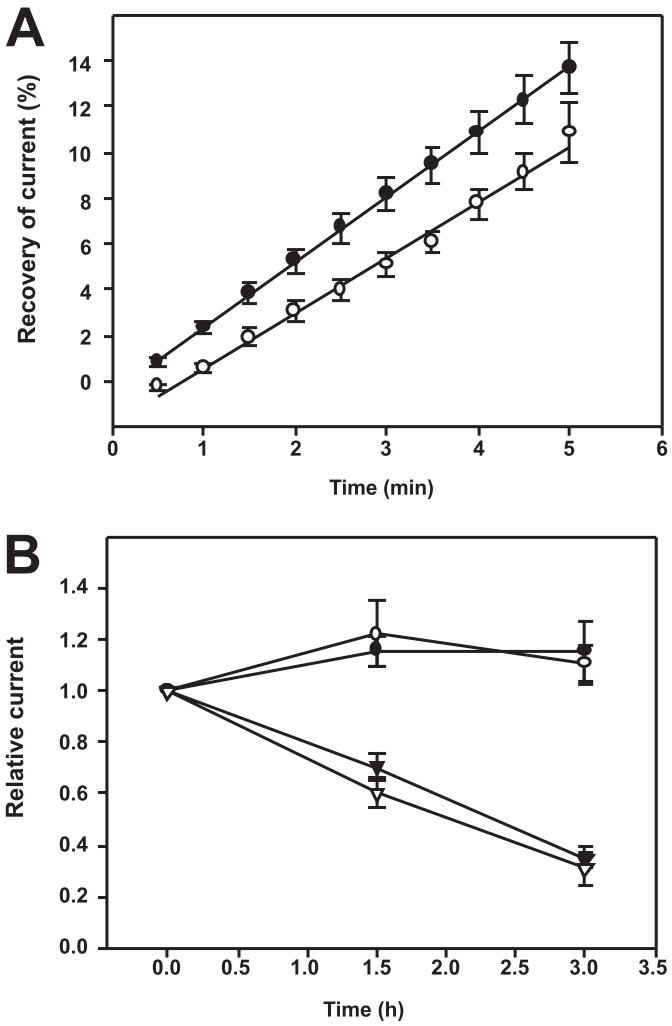

FIGURE 4. **ENaC exocytosis and endocytosis are not affected by the βC43A,C557A mutation.** *A*, oocytes were injected with cRNA for αS583Cβγ (*closed circles*) or the mutant αS583CβC43A,C557Aγ (*open circles*). Surface ENaC activity was blocked with MTSET and current recovery was monitored over time and plotted as the percentage of amiloride-sensitive whole cell current prior to MTSET treatment. Rates of current recovery were 2.84 ± 0.02% min^{-1} (*closed circles*, $n = 9$) and 2.42 ± 0.08% min^{-1} (*open circles*, $n = 21$). There was no significant difference in the rates of current recovery. *B*, oocytes were injected with cRNA for αβγ (*closed symbols*) or the mutant αβC43A,C557Aγ (*open symbols*). Amiloride-sensitive currents were measured in oocytes up to 3 h with (*triangles*) or without (*circles*) addition of brefeldin A to block delivery of channels from the biosynthetic pathway to the plasma membrane ($n = 9–12$ oocytes). There was no significant difference in current reductions in response to brefeldin A.

the change to a high [Na^+] solution, Na^+ currents rapidly rise to a peak current (I_{peak}), followed by a decay to a steady-state current (I_{ss}). The ratio of I_{ss}/I_{peak} reflects the magnitude of the Na^+ self-inhibition response, with a smaller value indicating greater Na^+ self-inhibition. We found that ENaC with the βC43A,C557A mutant had a significantly greater Na^+ self-inhibition response when compared with WT ENaC (Fig. 5*B*, $p < 0.02$, $n = 16–18$), suggesting that mutating sites of β subunit palmitoylation reduced channel P_o.

To directly assess whether ENaCs lacking sites for β subunit palmitoylation have a reduced channel Po, oocytes expressing WT or αβC43A,C557Aγ channels were subjected to cell-attached patch clamp. As shown in Fig. 5, *C–E*, WT ENaC expressed in oocytes exhibited an intermediate P_o of 0.45 ± 0.08, whereas αβC43A,C557Aγ channels had a significantly lower P_o (0.17 ± 0.06; $p < 0.05$, $n = 6$). Interestingly, the unitary Na^+ conductance of αβC43A,C557Aγ (5.1 ± 0.1 pS) was modestly, but significantly greater than WT conductance (4.2 ± 0.1 pS) ($p < 0.001$, $n = 4$).

The β Subunit C43A,C557A Mutation Does Not Alter the Extent of α or γ Subunit Cleavage—We previously reported that α subunit cleavage at two sites by the protease furin, as well as γ subunit cleavage by furin and a second protease, activates ENaC by releasing inhibitory tracts and increasing channel P_o (53, 55). We examined whether the reduced P_o of channels lacking sites for β subunit palmitoylation reflected a reduced fraction of cleaved channel at the cell surface. Oocytes expressing WT or αβC43A,C557Aγ channels and either a C-terminal V5 epitope-tagged α or γ subunit were treated with the membrane-impermeant sulfo-NHS-SS-biotin. Cell surface (biotinylated) ENaCs were recovered with streptavidin-conjugated agarose and subjected to immunoblotting with anti-V5 antibodies to reveal the full-length α (95 kDa) or γ (93 kDa) subunits, as well as the cleaved α (65 kDa) or γ (75 kDa) forms (Fig. 6*A*). Our results in Fig. 6, *A* and *B*, showed that the fraction of cleaved α and γ was not significantly altered by blocking palmitoylation of βC43 and βC557 ($p = 0.59$ for α, and $p = 0.16$ for γ).

DISCUSSION

Palmitoylation of Ion Channels Has Diverse Functional Effects—There are few reports of Cys palmitoylation of ion channels. The functional consequences of channel palmitoylation are diverse and include effects on channel activity, membrane trafficking, and stability. For example, PKA-dependent phosphorylation and inhibition of large conductance calcium- and voltage-gated potassium (BK) channels is dependent on Cys palmitoylation of two key Cys residues within the Cys-rich STREX (stress regulated exon) domain of the cytoplasmic C terminus of the pore-forming α subunit (59). Palmitoylation of the STREX domain results in channel activation and enhances the association of the C-terminal tail of the α subunit with the plasma membrane. In contrast, PKA-mediated phosphorylation of an adjacent Ser within the same subunit of the tetrameric structure inhibits channel activity as well as the interaction of the channel's C terminus with the plasma membrane. The GluR6 kainate receptor, a ligand-gated ion channel, is palmitoylated on two cytoplasmic Cys residues (60). Cells expressing receptors with mutations of these Cys residues exhibited normal kainate-dependent currents and similar levels of receptors, but PKC-dependent phosphorylation of the mutant channel in an *in vitro* assay was 2.7-fold greater than for the WT channel, suggesting that palmitoylation could regulate receptor activity by modulating the phosphorylation state of the channel.

Cys palmitoylation can directly alter channel activity. For example, voltage-gated N-type Ca^{2+} channels are modulated by diverse β subunits such that co-expression of the channel with CaVβ1b, CaVβ3, or CaVβ4 results in channel inhibition by either M1 or neurokinin-1 receptors, or by exogenous arachidonic acid (61, 62). Co-expression of the channel with the CaVβ2a subunit blocks neurokinin-1 receptor- or arachidonic acid-mediated inhibition. The lack of channel inhibition was

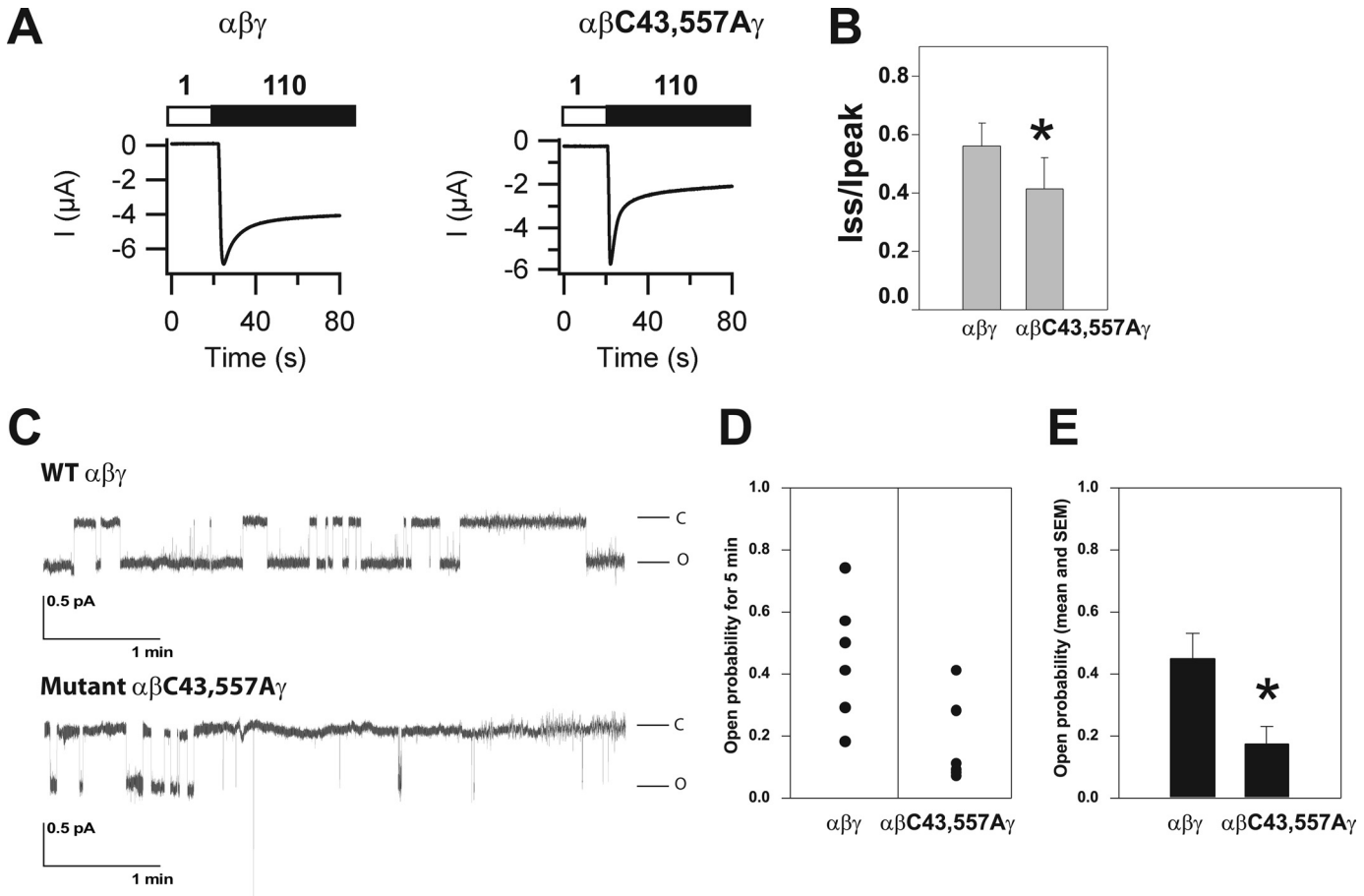

FIGURE 5. **ENaCs with the βC43A,C557A mutation exhibit reduced P_o.** *A*, Na^+ self-inhibition was assessed in oocytes expressing WT αβγ or the mutant αβC43A,C557Aγ. Whole cell currents were measured with oocytes bathed in a low [Na^+] solution (*white bar*, 1 mM Na^+ (sodium was replaced with *N*-methyl-D-glucamine)) and subsequently bathed in a high [Na^+] solution (*black bar*, 110 mM Na^+). Representative current tracings are shown. *B*, the ratios of the steady state (I_{ss}) to peak (I_{peak}) currents reflect the extent of the Na^+ self-inhibition response (mean ± S.E., *, $p < 0.02$, $n = 16–18$). *C–E*, cell attached patch clamp recordings were obtained from oocytes expressing αβγ or αβC43A,C557Aγ. Patches were clamped at −100 mV (membrane potential). Both bath and pipette solutions contained 110 mM Na^+. Recordings containing single channels lasting for at least 5 min were selected for analysis. Representative recordings of single channel currents are shown in *C* where the *letters C* and *O* represent closed and open states, respectively. The *scale bars* indicate current amplitude (pA) and time (minutes). P_o was determined as described under "Experimental Procedures" and presented in *D* for multiple experiments ($n = 6$) and as the mean ± S.E. in *E*. The P_o for αβC43A,C557Aγ (0.17 ± 0.06) was significantly lower than that determined for WT αβγ (0.45 ± 0.08) (*, $p = 0.02$, $n = 6$).

dependent on palmitoylation of CaVβ2a. The voltage-dependent potassium channel Kv1.1 is palmitoylated on a cytoplasmic Cys within the S2–S3 linker domain. Blocking palmitoylation with a Cys mutation reduced voltage sensing by the channel. Palmitoylation may also enhance surface expression of Kv1.1 (42).

Cys palmitoylation alters the activity of voltage-dependent Kv1.5 channels by affecting their trafficking (42, 64). Kv1.5 is palmitoylated on its cytosolic C terminus at one site (64). Channels with a Cys mutation exhibited enhanced surface expression due to a slower rate of internalization but exhibited no change in the voltage dependence of channel activation. The ATP-gated cationic P2X7 channel is palmitoylated on multiple Cys within its cytosolic C-terminal tail. Mutation of multiple clusters of Cys found 150–250 residues away from the transmembrane domain-blocked channel palmitoylation and reduced its cell surface expression (33). The mutant P2X7 channels exhibited reduced association with detergent-resistant membrane domains, shorter half-lives, and were retained in the endoplasmic reticulum. Furthermore, Cys palmitoylation influences the ability of aquaporin-4 channels to assemble tetramers into clusters referred to as orthogonal arrays (65, 66).

Palmitoylation of ENaC Modulates Channel Gating—We used fatty acid-exchange chemistry to assess Cys palmitoylation of ENaC subunits, as our attempts to label ENaC subunits with [^{3}H]palmitate were not successful (data not shown). Our success with the fatty acid-exchange assay likely reflects the greater sensitivity of detecting biotinylated subunits when compared with the detection of subunits labeled with [^{3}H]palmitate. Despite the presence of multiple cytoplasmic Cys residues in each subunit, we observed palmitoylation of only the β and γ subunits. Subsequent analyses of β subunit cytoplasmic Cys mutants revealed that the two Cys residues adjacent to M1 and M2 are palmitoylated. The placement of palmitate in proximity to the transmembrane domains is consistent with sites of palmitoylation that have been described for other transmembrane proteins (29). Our results suggest that Cys palmitoylation of the β subunit does not modulate channel membrane trafficking or levels of cell surface expression. Instead, our data indicate that Cys palmitoylation has a role in

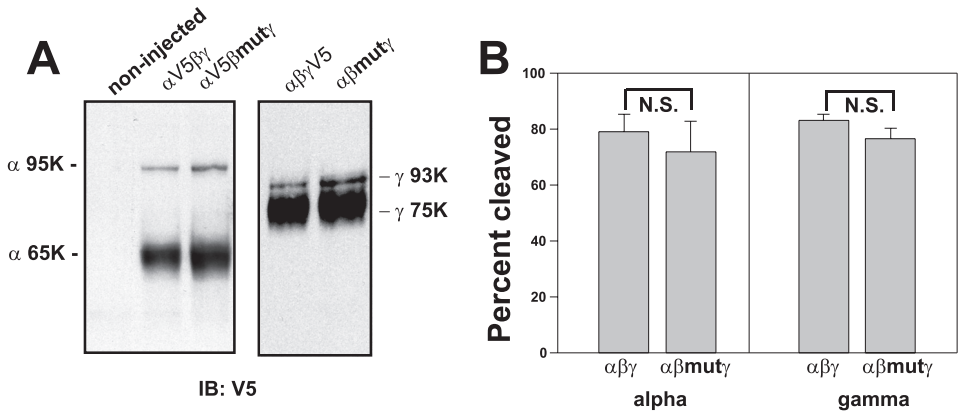

FIGURE 6. **Cleavage of ENaC is not affected by the βC43A,C557A mutation.** Oocytes ($n = 30–40$ per lane) expressing WT αβγ or αβC43A,C557Aγ (*βmut*) with an epitope-tagged α or γ subunit (N-terminal HA and C-terminal V5) were biotinylated and solubilized. Biotin-labeled proteins were precipitated and subjected to immunoblotting with anti-V5 antibodies. *A*, the mobility of the immature non-cleaved (α 95K and γ 93K) and mature cleaved (α 65K and γ 75K) subunits are indicated for a representative immunoblot. *B*, data from 3 experiments (1–2 frogs and 30–40 oocytes each) are presented as the percent cleaved α or γ subunit. There was no significant (*N.S.*) difference between the percentage of cleaved α or γ subunit in ENaCs containing WT β (% cleaved α, 79.2 ± 6.0, $n = 5$; % cleaved γ, 83.8 ± 2.1, $n = 6$) or mutant βC43A,C557A (% cleaved α, 71.9 ± 11.0, $n = 6$; % cleaved γ, 76.5 ± 4.0, $n = 6$).

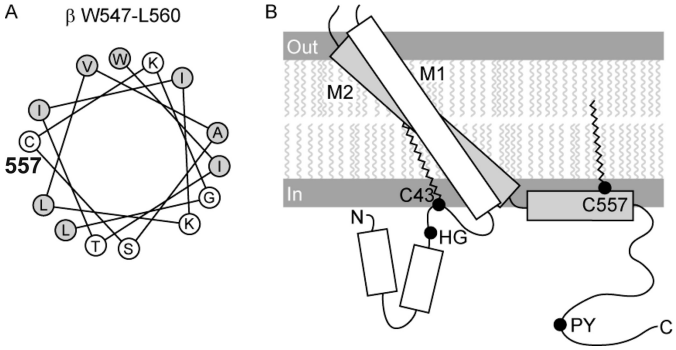

FIGURE 7. **Predicted locations of palmitoylated βC43 and βC557.** The presence of α-helices in the cytoplasmic domains was predicted using the PROF program of cascaded multiple classifiers to predict secondary structure (available on-line). *A*, palmitoylated βC557 is within an α-helix at the junction of the C-terminal cytoplasmic domain and M2. Placement of residues in the C-terminal cytoplasmic α-helix is shown as a helical wheel. Hydrophobic residues are indicated by *shaded circles*; hydrophilic residues are indicated by *open circles*. See text for discussion. *B*, *rectangles* represent α-helices. The *rotation*, *angle*, and *length* of the *rectangles* for M1 and M2 are based on the crystal structure of ASIC1. Palmitoylated βC43 in the N-terminal cytoplasmic domain is found in a coil domain between M1 and a cytoplasmic α-helix. The His-Gly (*HG*) and Pro-Tyr (*PY*) motifs are located at the indicated positions. Palmitate is indicated within the inner leaflet of the membrane as *wavy lines*.

modulating ENaC gating, possibly by enhancing interactions of the β subunit's cytoplasmic domains with the plasma membrane.

To understand how Cys palmitoylation of the β subunit might affect ENaC gating, we generated a model of the transmembrane domains and cytoplasmic domains of the β subunit (Fig. 7). The rotation, angle, length, and α-helical structure of the two transmembrane domains were based on the published crystal structure of ASIC1 (67). M1 includes βA50-βI71 and M2 includes βI513-βI546. We used the PROF program of cascaded multiple classifiers to predict the secondary structure of the N-terminal and C-terminal cytoplasmic domains (68). Two distinct α-helices are predicted within the β N-terminal cytoplasmic domain (βV3-R13 and βY22-C30), and one α-helix is predicted to be within the β C-terminal cytoplasmic domain (βW547-R562). Intervening sequences are predicted to be coil. The palmitoylated residue βC557 is located within the α-helix βW547-R562 adjacent to M2 (βI513-βI546), whereas palmitoylated residue βC43 is located in a loop between the second α-helix (βY22-C30) and M1 (βA50-βI71). Analysis of βW547-L560 on a helical wheel places hydrophobic residues and palmitoylated βC557 on one side and polar and charged residues primarily on the other side of the α-helix (Fig. 7). This suggests that the βW547-R562 α-helix is amphipathic and naturally associated with the membrane. Palmitoylation of βC557 would thereby enhance the hydrophobicity and membrane association of the C-terminal cytoplasmic domain.

Other factors that may influence the interactions of ENaC cytoplasmic domains with the plasma membrane have also been reported to affect ENaC gating. For example, increases in levels of specific inositol phospholipids increase channel P_o. These negatively charged lipids appear to enhance interactions of specific cytoplasmic domains of ENaC subunits with the plasma membrane. Deletion of the tract βK552-R563 (and a similar tract in γ, but not α) was reported to block PI3K stimulation of mouse ENaC activity by co-expression in CHO cells (23). Furthermore, deletion of the basic tract βK4-K16 at the extreme N terminus of mouse ENaC blocked both the down-regulation of channel activity in CHO cells upon depletion of membrane phosphatidylinositol 4,5 bisphosphate, and the increase in P_o due to application of exogenous phosphatidylinositol 4,5 bisphosphate (23). The highly conserved His-Gly motif (βHG37) is found adjacent to the palmitoylation site at βC43. The His-Gly motif is conserved in α, β, and γ subunits across species (69). The βG37S mutation in human ENaC is associated with pseudohypoaldosteronism, and ENaC containing βG37S exhibits a significantly reduced P_o of 0.04, compared with a P_o of 0.48 for WT ENaC (69). Kellenberger *et al.* (70) previously reported that multiple Cys in the N- and C-terminal cytoplasmic domains, but not Cys in M1 or M2 of ENaC expressed in cut-open *Xenopus* oocytes, were responsible for thiol-mediated inhibition of ENaC by a variety of reagents. Because Cys palmitoylation is reversible, thiol-mediated inhibition could proceed by blocking ENaC palmitoylation. As noted above, βC557 is likely within an α-helix contiguous with M2, and palmitoylation at this site could have a direct impact on the channel pore. In support of this possibility, we found that ENaCs with a βC43A,C557A mutation had a significantly reduced P_o and a significantly increased unitary conductance when compared with WT channels, indicating that palmitoylation alters the structure of the conducting pore.

Protein palmitoylation can impact protein-lipid interactions, and there are reports that ENaC is present in cholesterol-en-

riched lipid rafts in both amphibian A6 cells and mouse cortical collecting duct cells (10, 71). Hill *et al.* (10) reported that treatment of cortical collecting duct cells with apical β-cyclodextrin reduced ENaC currents by blocking constitutive apical biosynthetic delivery, but we did not observe an effect on biosynthetic delivery of ENaC in *Xenopus* oocytes due to mutation of βC43,C557. Alternatively, βC43 or βC557 palmitoylation could influence protein-protein interactions within the cytoplasm by altering the association or orientation of the cytoplasmic tails with the lipid bilayer, making motifs more or less available for interactions. Because we did not find that ENaC with mutant βC43A,C557A had altered membrane trafficking, it is unlikely that palmitoylation of the β subunit influences ENaC binding of Nedd4-2 at the PY motif in the C-terminal tail (Fig. 7) that regulates ENaC endocytosis and recycling at the cell surface (63). For the same reason, it is unlikely that β subunit palmitoylation affects coat protein complex II binding to αRSRYW620 and thereby ER exit (7).

Palmitoylation of the α subunit was not detected with our assay using fatty acid-exchange chemistry to assess Cys palmitoylation. However, a background level of palmitoylation was seen with the βC30A,C43A,C557A,C595A mutant (Figs. 1 and 2). It is likely that this background does not represent palmitoylation of βC10, because the βC10A mutation did not reduce levels of β subunit palmitoylation when compared with WT (Fig. 2). The background may reflect palmitoylation of residues βC61 in M1 and/or βC533 in M2. The extracellular domain of the β subunit also contains two unique Cys residues (βC182 and βC187) that are conserved in all mammalian β subunits, but not found in α or γ subunits. It is possible that βC182 and βC187 could be differentially accessible to modification with biotin in our assay. Interestingly, the βC43 residue is conserved in mammalian α and β ENaC subunits, but not in the γ subunit. Although the βC557 residue is present in mouse and rat, it is not conserved in mammalian α, β, or γ subunits. Although we did observe palmitoylation of the γ subunit, we have not yet determined the sites and functional consequences of palmitoylation of this subunit.

Our results also suggest that only 4% to 5% of the cellular pool of ENaC is modified by β subunit palmitoylation, raising the possibility that ENaC palmitoylation occurs at selected site(s) within the cell. Because mutations that prevent β subunit palmitoylation affect channel gating, it is likely that the cell surface represents one cellular compartment where channels are modified by palmitoylation. Furthermore, it is interesting to note that the unitary Na^+ conductance of channels that lacked β subunit palmitoylation (5.1 ± 0.1 pS) was significantly greater than that observed for WT (4.2 ± 0.1 pS). Because WT channels expressed in oocytes exhibit a consistent Na^+ conductance that in our studies is ~4 pS, it is likely that the vast majority of channels at the plasma membrane of oocytes have β subunits that are palmitoylated.

It is also notable that the Cys residues we identified as sites of β subunit palmitoylation do not appear to exert functional effects in an independent manner. Mutation of only one of the Cys residues was sufficient to reduce levels of β subunit palmitoylation to background (Fig. 2). Furthermore, we did not observe an additive effect on the reduction of ENaC currents in channels bearing mutations of βC43 or βC557, when compared with ENaC with a double mutation at βC43 and βC557. Our results suggest that preventing palmitoylation at one site by an introduced mutation may reduce palmitoylation at the second site.

In summary, we have identified sites of palmitoylation of ENaC in the cytoplasmic domains of the β subunit of ENaC. These sites are in proximity to the two transmembrane domains of ENaC. Channels with mutations that prevent β subunit palmitoylation at these two sites have reduced activity reflecting a reduced channel P_o. We suggest that β subunit palmitoylation enhances interactions of ENaC cytoplasmic tails with the plasma membrane, resulting in conformation changes in the channel's pore and gate that favors the open state of the channel.

Acknowledgment—We thank Paul A. Poland for technical assistance.

REFERENCES

1. Chen, C. C., England, S., Akopian, A. N., and Wood, J. N. (1998) *Proc. Natl. Acad. Sci. U.S.A.* **95,** 10240–10245
2. Jasti, J., Furukawa, H., Gonzales, E. B., and Gouaux, E. (2007) *Nature* **449,** 316–323
3. Valentijn, J. A., Fyfe, G. K., and Canessa, C. M. (1998) *J. Biol. Chem.* **273,** 30344–30351
4. May, A., Puoti, A., Gaeggeler, H. P., Horisberger, J. D., and Rossier, B. C. (1997) *J. Am. Soc. Nephrol.* **8,** 1813–1822
5. Weisz, O. A., Wang, J. M., Edinger, R. S., and Johnson, J. P. (2000) *J. Biol. Chem.* **275,** 39886–39893
6. Alvarez de la Rosa, D., Li, H., and Canessa, C. M. (2002) *J. Gen. Physiol.* **119,** 427–442
7. Mueller, G. M., Kashlan, O. B., Bruns, J. B., Maarouf, A. B., Aridor, M., Kleyman, T. R., and Hughey, R. P. (2007) *J. Biol. Chem.* **282,** 33475–33483
8. Hughey, R. P., Mueller, G. M., Bruns, J. B., Kinlough, C. L., Poland, P. A., Harkleroad, K. L., Carattino, M. D., and Kleyman, T. R. (2003) *J. Biol. Chem.* **278,** 37073–37082
9. Hughey, R. P., Bruns, J. B., Kinlough, C. L., Harkleroad, K. L., Tong, Q., Carattino, M. D., Johnson, J. P., Stockand, J. D., and Kleyman, T. R. (2004) *J. Biol. Chem.* **279,** 18111–18114
10. Hill, W. G., Butterworth, M. B., Wang, H., Edinger, R. S., Lebowitz, J., Peters, K. W., Frizzell, R. A., and Johnson, J. P. (2007) *J. Biol. Chem.* **282,** 37402–37411
11. Hughey, R. P., Bruns, J. B., Kinlough, C. L., and Kleyman, T. R. (2004) *J. Biol. Chem.* **279,** 48491–48494
12. Kleyman, T. R., Carattino, M. D., and Hughey, R. P. (2009) *J. Biol. Chem.* **284,** 20447–20451
13. Passero, C. J., Hughey, R. P., and Kleyman, T. R. (2010) *Curr. Opin. Nephrol. Hypertens.* **19,** 13–19
14. Ovaere, P., Lippens, S., Vandenabeele, P., and Declercq, W. (2009) *Trends Biochem. Sci.* **34,** 453–463
15. Rossier, B. C., and Stutts, M. J. (2009) *Annu. Rev. Physiol.* **71,** 361–379
16. Butterworth, M. B., Weisz, O. A., and Johnson, J. P. (2008) *J. Biol. Chem.* **283,** 35305–35309
17. Hamm, L. L., Feng, Z., and Hering-Smith, K. S. (2010) *Curr. Opin. Nephrol. Hypertens.* **19,** 98–105
18. Butterworth, M. B., Edinger, R. S., Ovaa, H., Burg, D., Johnson, J. P., and Frizzell, R. A. (2007) *J. Biol. Chem.* **282,** 37885–37893
19. Ruffieux-Daidié, D., Poirot, O., Boulkroun, S., Verrey, F., Kellenberger, S., and Staub, O. (2008) *J. Am. Soc. Nephrol.* **19,** 2170–2180
20. Knight, K. K., Olson, D. R., Zhou, R., and Snyder, P. M. (2006) *Proc. Natl. Acad. Sci. U.S.A.* **103,** 2805–2808
21. Pochynyuk, O., Staruschenko, A., Tong, Q., Medina, J., and Stockand, J. D. (2005) *J. Biol. Chem.* **280,** 37565–37571
22. Pochynyuk, O., Tong, Q., Staruschenko, A., Ma, H. P., and Stockand, J. D.

(2006) *Am. J. Physiol. Renal Physiol.* **290,** F949–F957
23. Pochynyuk, O., Tong, Q., Medina, J., Vandewalle, A., Staruschenko, A., Bugaj, V., and Stockand, J. D. (2007) *J. Gen. Physiol.* **130,** 399–413
24. Pochynyuk, O., Bugaj, V., Vandewalle, A., and Stockand, J. D. (2008) *Am. J. Physiol. Renal Physiol.* **294,** F38–F46
25. Yue, G., Malik, B., Yue, G., and Eaton, D. C. (2002) *J. Biol. Chem.* **277,** 11965–11969
26. Pochynyuk, O., Tong, Q., Staruschenko, A., and Stockand, J. D. (2007) *J. Physiol.* **580,** 365–372
27. Fernández-Hernando, C., Fukata, M., Bernatchez, P. N., Fukata, Y., Lin, M. I., Bredt, D. S., and Sessa, W. C. (2006) *J. Cell Biol.* **174,** 369–377
28. Tsutsumi, R., Fukata, Y., and Fukata, M. (2008) *Pflugers Arch.* **456,** 1199–1206
29. Linder, M. E., and Deschenes, R. J. (2007) *Nat. Rev. Mol. Cell. Biol.* **8,** 74–84
30. Fang, C., Deng, L., Keller, C. A., Fukata, M., Fukata, Y., Chen, G., and Lüscher, B. (2006) *J. Neurosci.* **26,** 12758–12768
31. Lam, K. K., Davey, M., Sun, B., Roth, A. F., Davis, N. G., and Conibear, E. (2006) *J. Cell Biol.* **174,** 19–25
32. Mulugeta, S., and Beers, M. F. (2003) *J. Biol. Chem.* **278,** 47979–47986
33. Gonnord, P., Delarasse, C., Auger, R., Benihoud, K., Prigent, M., Cuif, M. H., Lamaze, C., and Kanellopoulos, J. M. (2009) *FASEB J.* **23,** 795–805
34. Qanbar, R., and Bouvier, M. (2003) *Pharmacol. Ther.* **97,** 1–33
35. Valdez-Taubas, J., and Pelham, H. (2005) *EMBO J.* **24,** 2524–2532
36. Yik, J. H., Saxena, A., Weigel, J. A., and Weigel, P. H. (2002) *J. Biol. Chem.* **277,** 40844–40852
37. Alvarez, E., Gironès, N., and Davis, R. J. (1990) *J. Biol. Chem.* **265,** 16644–16655
38. Kinlough, C. L., McMahan, R. J., Poland, P. A., Bruns, J. B., Harkleroad, K. L., Stremple, R. J., Kashlan, O. B., Weixel, K. M., Weisz, O. A., and Hughey, R. P. (2006) *J. Biol. Chem.* **281,** 12112–12122
39. Yang, X., Kovalenko, O. V., Tang, W., Claas, C., Stipp, C. S., and Hemler, M. E. (2004) *J. Cell Biol.* **167,** 1231–1240
40. Hérincs, Z., Corset, V., Cahuzac, N., Furne, C., Castellani, V., Hueber, A. O., and Mehlen, P. (2005) *J. Cell Sci.* **118,** 1687–1692
41. Lefkowitz, R. J., and Shenoy, S. K. (2005) *Science* **308,** 512–517
42. Gubitosi-Klug, R. A., Mancuso, D. J., and Gross, R. W. (2005) *Proc. Natl. Acad. Sci. U.S.A.* **102,** 5964–5968
43. Ahn, Y. J., Brooker, D. R., Kosari, F., Harte, B. J., Li, J., Mackler, S. A., and Kleyman, T. R. (1999) *Am. J. Physiol.* **277,** F121–F129
44. Drisdel, R. C., and Green, W. N. (2004) *BioTechniques* **36,** 276–285
45. Drisdel, R. C., Alexander, J. K., Sayeed, A., and Green, W. N. (2006) *Methods* **40,** 127–134
46. Bruns, J. B., Baofeng, H., Ahn, Y. J., Sheng, S., Hughey, R. P., and Kleyman, T. R. (2003) *Am. J. Physiol. Renal Physiol.* **285,** F600–F609
47. Carattino, M. D., Hill, W. G., and Kleyman, T. R. (2003) *J. Biol. Chem.* **278,** 36202–36213
48. Carattino, M. D., Sheng, S., Bruns, J. B., Pilewski, J. M., Hughey, R. P., and Kleyman, T. R. (2006) *J. Biol. Chem.* **281,** 18901–18907
49. Snyder, P. M., Olson, D. R., and Bucher, D. B. (1999) *J. Biol. Chem.* **274,** 28484–28490
50. Kashlan, O. B., Mueller, G. M., Qamar, M. Z., Poland, P. A., Ahner, A., Rubenstein, R. C., Hughey, R. P., Brodsky, J. L., and Kleyman, T. R. (2007) *J. Biol. Chem.* **282,** 28149–28156
51. Harris, M., Firsov, D., Vuagniaux, G., Stutts, M. J., and Rossier, B. C. (2007) *J. Biol. Chem.* **282,** 58–64
52. Bruns, J. B., Carattino, M. D., Sheng, S., Maarouf, A. B., Weisz, O. A., Pilewski, J. M., Hughey, R. P., and Kleyman, T. R. (2007) *J. Biol. Chem.* **282,** 6153–6160
53. Sheng, S., Carattino, M. D., Bruns, J. B., Hughey, R. P., and Kleyman, T. R. (2006) *Am. J. Physiol. Renal Physiol.* **290,** F1488–F1496
54. Carattino, M. D., Sheng, S., and Kleyman, T. R. (2005) *J. Biol. Chem.* **280,** 4393–4401
55. Maarouf, A. B., Sheng, N., Chen, J., Winarski, K. L., Okumura, S., Carattino, M. D., Boyd, C. R., Kleyman, T. R., and Sheng, S. (2009) *J. Biol. Chem.* **284,** 7756–7765
56. Snyder, P. M., Bucher, D. B., and Olson, D. R. (2000) *J. Gen. Physiol.* **116,** 781–790
57. Carattino, M. D., Edinger, R. S., Grieser, H. J., Wise, R., Neumann, D., Schlattner, U., Johnson, J. P., Kleyman, T. R., and Hallows, K. R. (2005) *J. Biol. Chem.* **280,** 17608–17616
58. Sheng, S., McNulty, K. A., Kieber-Emmons, T., and Kleyman, T. R. (2001) *J. Biol. Chem.* **276,** 1326–1334
59. Tian, L., Jeffries, O., McClafferty, H., Molyvdas, A., Rowe, I. C., Saleem, F., Chen, L., Greaves, J., Chamberlain, L. H., Knaus, H. G., Ruth, P., and Shipston, M. J. (2008) *Proc. Natl. Acad. Sci. U.S.A.* **105,** 21006–21011
60. Pickering, D. S., Taverna, F. A., Salter, M. W., and Hampson, D. R. (1995) *Proc. Natl. Acad. Sci. U.S.A.* **92,** 12090–12094
61. Qin, N., Platano, D., Olcese, R., Costantin, J. L., Stefani, E., and Birnbaumer, L. (1998) *Proc. Natl. Acad. Sci. U.S.A.* **95,** 4690–4695
62. Heneghan, J. F., Mitra-Ganguli, T., Stanish, L. F., Liu, L., Zhao, R., and Rittenhouse, A. R. (2009) *J. Gen. Physiol.* **134,** 369–384
63. Malik, B., Price, S. R., Mitch, W. E., Yue, Q., and Eaton, D. C. (2006) *Am. J. Physiol. Renal Physiol.* **290,** F1285–F1294
64. Jindal, H. K., Folco, E. J., Liu, G. X., and Koren, G. (2008) *Am. J. Physiol. Heart Circ. Physiol.* **294,** H2012–H2021
65. Suzuki, H., Nishikawa, K., Hiroaki, Y., and Fujiyoshi, Y. (2008) *Biochim. Biophys. Acta* **1778,** 1181–1189
66. Crane, J. M., and Verkman, A. S. (2009) *Biophys. J.* **97,** 3010–3018
67. Gonzales, E. B., Kawate, T., and Gouaux, E. (2009) *Nature* **460,** 599–604
68. Ouali, M., and King, R. D. (2000) *Protein Sci.* **9,** 1162–1176
69. Gründer, S., Firsov, D., Chang, S. S., Jaeger, N. F., Gautschi, I., Schild, L., Lifton, R. P., and Rossier, B. C. (1997) *EMBO J.* **16,** 899–907
70. Kellenberger, S., Gautschi, I., Pfister, Y., and Schild, L. (2005) *J. Biol. Chem.* **280,** 7739–7747
71. Hill, W. G., An, B., and Johnson, J. P. (2002) *J. Biol. Chem.* **277,** 33541–33544